(1977) and the dideoxyribonucleotide terminator method of Sanger et al. (1977). For reliable sequencing, the one-lane method will be more dependent on confirmation by sequencing of the complementary strand. The method should be particularly useful in routine sequencing applications, as in identification of known sequences, confirmation of known sequences, or in comparative sequencing of mutant DNAs. Work to extend and refine this approach is proceeding in our laboratory.

ACKNOWLEDGMENTS

We are indebted to Lee F. Johnson, John N. Reeve, Elio F. Vanin, Sylvia Perryman, Cynthia Rossano, Rell W. Ambrose, and Paul Anziano for generous help and advice.

Registry No. Piperidine, 110-89-4.

REFERENCES

Albert, A., & Brown, D. J. (1954) *J. Chem. Soc.*, 2060-2071.

Brownlee, G. G., & Sanger, F. (1967) *J. Mol. Biol. 23*, 337-353.

Jones, A. S., Mian, A. M., & Walker, R. T. (1966) *J. Chem. Soc. C*, 1784-1786.

Maxam, A. L., & Gilbert, W. (1977) *Proc. Natl. Acad. Sci. U.S.A. 74*, 560-564.

Maxam, A. L., & Gilbert, W. (1980) *Methods Enzymol. 65*, 499-560.

Pless, R. C., & Bessman, M. J. (1983) *Biochemistry 22*, 4905-4915.

Sanger, F., Nicklen, S., & Coulson, A. R. (1977) *Proc. Natl. Acad. Sci. U.S.A. 74*, 5463-5467.

Sealey, P. G., & Southern, E. M. (1982) in *Gel Electrophoresis of Nucleic Acids: A Practical Approach* (Rickwood, R., & Hames, B. D., Eds.) pp 52-53, IRL Press Limited, Oxford and Washington, DC.

Southern, E. M. (1979) *Anal. Biochem. 100*, 319-323.

Sutcliffe, J. G. (1979) *Cold Spring Harbor Symp. Quant. Biol. 43*, 77-90.

Internal Motions in B- and Z-Form Poly(dG-dC)·Poly(dG-dC): ^{1}H NMR Relaxation Studies†

Peter A. Mirau,‡ Ronald W. Behling, and David R. Kearns*

Department of Chemistry, University of California—San Diego, La Jolla, California 92093

Received December 31, 1984; Revised Manuscript Received May 31, 1985

ABSTRACT: Proton NMR relaxation measurements are used to compare the molecular dynamics of 60 base pair duplexes of B- and Z-form poly(dG-dC)·poly(dG-dC). The relaxation rates of the exchangeable guanine imino protons (G_{im}) in H_2O and in 90% D_2O show that below 20 °C spin–lattice relaxation is exclusively from proton–proton magnetic dipolar interactions while proton–nitrogen interactions contribute about 30% to the spin–spin relaxation. The observation that the spin–lattice relaxation is nonexponential and that the initial spin–lattice relaxation rate of the G_{im}, G-H8 and C-H6 protons depends on the selectivity of the exciting pulse shows that spin–diffusion dominates the spin–lattice relaxation. The relaxation rates of the G_{im}, C-H5, and C-H6 in B- and Z-form poly(dG-dC)·poly(dG-dC) cannot be explained by assuming the DNA behaves as a rigid rod. The data can be fit by assuming large-amplitude out of plane motions (±30–40°, τ = 1–100 ns) and fast, large-amplitude local torsional motions (±25–90°, τ = 0.1–1.5 ns) in addition to collective torsional motions. The results for the B and Z forms show that the rapid internal motions are similar and large in both conformations although backbone motions are slightly slower, or of lower amplitude, in Z DNA. At high temperatures (>60 °C), imino proton exchange with solvent dominates the spin–lattice relaxation of B-form poly(dG-dC)·poly(dG-dC), but in the Z form no exchange contribution (<2 s^{-1}) is observed at temperatures as high as 85 °C. Conformational fluctuations that expose the imino protons to the solvent are strikingly different in the B and Z forms. The results obtained here are compared with those previously reported for poly(dA-dT)·poly(dA-dT).

There is considerable interest in the sequence-dependent properties of DNA and the possible role that conformational heterogeneity plays in the biological functions of DNA and the sequence specific recognition by proteins. Recent X-ray diffraction studies of single crystals of DNA oligonucleotides have revealed significant sequence effects on DNA conformation (Izatt et al., 1971; Williams, 1972; Wang et al., 1979, 1981; Wing et al., 1980) and suggested possible roles in the interaction of DNA with proteins (Dickerson & Drew, 1981; Dickerson, 1983; Rich et al., 1984). Transient fluctuations in the local conformation of the DNA may also play a role in moderating DNA–protein interactions and, if large enough, could significantly diminish the importance of sequence effects on the time-averaged conformations of the DNA. In addition to possible biochemical importance, an evaluation of internal motions in DNA is crucial to current efforts to use 1D and 2D NMR relaxation techniques to determine the structures of DNAs in solution (Early et al., 1980b; Tjerneld, 1982; Feigon et al., 1983a,b; Haasnoot et al., 1983; Keepers & James, 1984).

NMR studies have already been used to characterize the internal motions in the backbone of DNA and RNA. Phos-

† This work was supported by the National Science Foundation (Grant PCM-8303374 to D.R.K.).

‡ Present address: AT&T Bell Laboratories, Murray Hill, NJ 07974.

0006-2960/85/0424-6200$01.50/0

phorus NMR studies of synthetic DNA and RNA polymers show that the backbone phosphates experience large-amplitude fluctuations in the 0.5–2-ns time range that appear to be independent of the DNA conformation (single or double stranded, or wrapped around histones) (Bolton & James, 1979; Hogan & Jardetzky, 1980). ^{13}C NMR studies show that the internal-motion time constants of the ribose and deoxyribose sugars are slightly longer (1–6 ns) than those of the phosphate (Hogan & Jardetzky, 1980; Levy et al., 1981). Although backbone motions have been well studied, there is little NMR data on the conformational fluctuations of the DNA bases (Lown et al., 1978; Early & Kearns, 1979; Early et al., 1980b). Because direct interactions between the DNA bases and the protein may be involved in DNA–protein recognition, it is particularly important to characterize those internal motions that affect base motions, and several different spectroscopic techniques have been used for this purpose. Measurements of the decay of fluorescence polarization anisotropy of bound intercalating dyes (Barkley & Zimm, 1979; Millar et al., 1981; Magde et al., 1983; Thomas & Schurr, 1983; Ashikawa et al., 1984) and the EPR spectrum of spin-labeled DNA (Robinson et al., 1980) indicate that the DNA undergoes large-amplitude torsional motions about the helix axis with correlation times in the nanosecond range. The initial, rapid decay of the fluorescence emission anisotropy from a theoretical value of 0.40–0.32 within 2 ns has been attributed to wobble of the chromophore with an root mean square fluctuation of ±21° (Barkley & Zimm, 1979). Recent measurements of the ethidium fluorescence polarization anisotropy indicate that poly(dG-dC)·poly(dG-dC) is more flexible (factor of 4–6-fold change in torsion and bending force constants) in the Z form than in the B form (Ashikawa et al., 1984), but light scattering studies (Thomas & Bloomfield, 1983) indicate poly(dG-dC)·poly(dG-dC) is stiffer in the Z form than in the B form. Proton exchange (imino and amino protons) has also been used to monitor large-amplitude fluctuations in DNA structure occurring on a millisecond time scale (Teitelbaum & Englander, 1975a,b; Early et al., 1981a,b; Mirau & Kearns, 1983, 1984a).

To examine the motion of the DNA bases and to explore the effect of sequence and conformation on dynamic properties of DNAs, we have studied several repeating-sequence, synthetic DNA polymers (Kearns et al., 1981; Mirau & Kearns, 1983; Assa-Munt et al., 1984). Perhaps the most interesting simple-sequence DNA is poly(dG-dC)·poly(dG-dC) because it was the first molecule shown to be capable of adopting a left-handed Z conformation (Pohl & Jovin, 1972; Drew et al., 1980; Wang et al., 1981). While the role of Z DNA in vivo has yet to be established (Lafer et al., 1981; Nordheim et al., 1982; Hill & Stollar, 1983; Rich et al., 1984), differences in the physical properties of B and Z DNA may be important in recognition processes.

In the present study, proton relaxation measurements are used to examine the molecular dynamics of the B and Z forms of poly(dG-dC)·poly(dG-dC). We show that the spin–lattice relaxation rates are critically dependent on the nature of the exciting pulse and exploit this to investigate the motional properties. The results show that rapid internal motions (amplitudes and rates) in B and Z DNAs are similar, but the slower fluctuations that result in exchange of the imino protons are different for the B and Z conformations.

Materials and Methods

Sample Preparation. Poly(dG-dC)·poly(dG-dC) (lot 676-7) was obtained from P-L Biochemicals, and buffer reagents were obtained from Sigma Chemical Co. The size of the DNA was reduced by 6.5 h of sonication on an Ultrasonics W-375 sonicator on a 50% duty cycle at 0–5 °C in 0.25 M NaCl, 0.025 M sodium cacodylate, and 0.01 M ethylenediaminetetraacetic acid (EDTA), at pH 7.0. The samples were dialyzed, ethanol precipitated twice, dried, and dissolved in the appropriate buffer (Granot et al., 1982). The average size of the DNA, 60 ± 10 base pairs, was determined by electrophoresis on a 7% polyacrylamide gel against ^{32}P-labeled *Hae*III restriction fragments of pBR322.

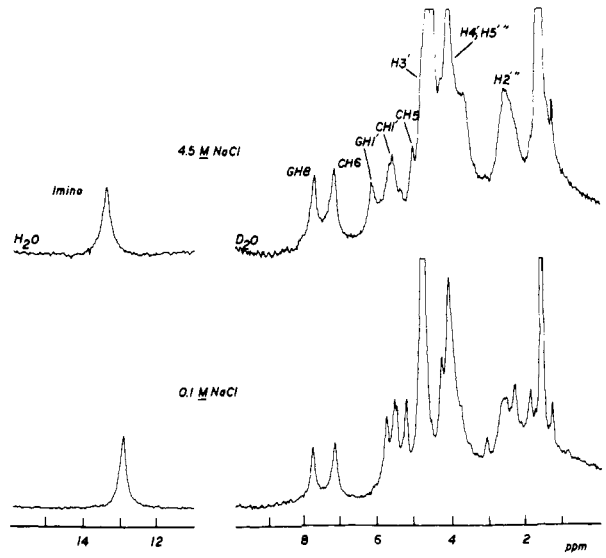

FIGURE 1: Proton spectra obtained at 20 °C and 360 MHz of Z-form (top) and B-form (bottom) poly(dG-dC)·poly(dG-dC). The imino spectra were obtained with a sample in H_2O, and the nonexchangeable proton spectra were obtained in D_2O.

NMR Methods. ^1H NMR spectra were obtained on a home-built 360-MHz Fourier-transform NMR spectrometer with a Nicolet 1280 computer. Semiselective spin–lattice and spin–spin relaxation rates for the imino protons were measured by the time-shared Redfield sequence (Wright et al., 1981) to apply the appropriate 90° and 180° pulses in the inversion recovery and Hahn spin-echo experiments. Nonselective spin–lattice relaxation rates in H_2O were measured by inverting all the resonances with a nonselective pulse, applying a homospoil pulse (50 ms) to randomize the transverse H_2O magnetization, and using a time-shared Redfield observe pulse. In D_2O, nonselective pulses were used to measure the spin–spin and nonselective spin–lattice relaxation rates. Selective spin–lattice relaxation rates were measured following a selective 180° (6-ms) "soft" pulse from the decoupler to the desired resonance. The decoupler pulse was audio modulated to simultaneously invert both the C-H5 and C-H6 resonances for measurement of the biselective relaxation rates.

Results

Relaxation Pathway. Dipolar relaxation may arise from several different types of proton–proton and proton–nitrogen interactions. Before analyzing the observed relaxation rates to extract information about internal motions, it is important to establish the internuclear interactions responsible for the relaxation, and in this section we briefly summarize the results of our two-dimensional (2D) NOE studies (Mirau & Kearns, 1984b) and present the effect of deuteration on the relaxation rates of the exchangeable imino protons.

(*A*) *Nonexchangeable Protons.* Figure 1 shows the 360-MHz proton spectrum of ~60 base pair fragments of poly(dG-dC)·poly(dG-dC) in H_2O and D_2O in the B and Z forms. Despite the large change in conformation, the spectra of the

Table I: Effect of Solvent Deuteration on the Dipolar Relaxation Rates of the Imino Protons of B-Form Poly(dG-dC)·Poly(dG-dC)[a]

relaxation rate measured	temp (°C)	rate (s^{-1}) in H_2O	rate (s^{-1}) in 90% D_2O
R_1^{ss}	20	15	1.6
R_2	20	106	37

[a] Values accurate to ±15%.

B and Z forms are remarkably similar (Patel et al., 1979, 1982; Dhingra et al., 1983). The most notable changes are that the imino and G-H1′ resonances shift slightly downfield in the Z form and the C-H2′ resonances shift into the main band containing the other H2′ and H2″ protons. The resonances in Z DNA are broader, partly because of the increased solvent viscosity at 4.5 M NaCl.

Proton-relaxation pathways in DNA can be determined by measuring 2D NOE spectra (Feigon et al., 1982; Mirau & Kearns, 1983, 1984b; Assa-Munt & Kearns, 1984), and the results relating to the dipolar relaxation of the B and Z forms of poly(dG-dC)·poly(dG-dC) are now summarized. Of the protons studied here, the strongest interaction in both B and Z forms is between the C-H5 and C-H6 protons, separated by 2.4 Å. In B-form DNA, the G-H8 proton interacts strongly with its own G-H2′ protons and, to a lesser extent, with the C-H2″ protons from the neighboring nucleotide on the same strand. About 20–30% of the C-H6 relaxation is from its interaction with the C-H2′ protons. In the Z form, G-H8 relaxation is dominated by interaction with the G-H1′ protons (Patel et al., 1982) because the guanine is in the syn conformation and the G-H8–C-H1′ distance is reduced from 3.7 to 2.2 Å (Wang et al., 1979).

(B) Imino Protons. The spin–lattice and spin–spin relaxation rates of the G_{im} may have contributions from both dipolar interactions with nearby amino protons and nitrogen atoms and from exchange of the imino protons with the solvent (Early et al., 1980b). In this section, we are specifically concerned with the dipolar contribution to relaxation, and the reported rates have been corrected for the exchange contribution (R_{ex} = 0.45 s^{-1} for B DNA at 25 °C and 0.0 s^{-1} for Z DNA) (Mirau & Kearns, 1984a). From the structure of the base pair, we expect the guanine imino protons to relax by interactions with the guanine and cytosine amino protons and with the guanine N1. Interactions between the five exchangeable protons with the remaining (nonexchangeable) protons in the molecule are expected to be much weaker because of the large interproton distances involved.

The contribution from the neighboring, exchangeable protons to the imino proton relaxation may be examined by changing the solvent from H_2O to 90% D_2O. Since deuterons are much less efficient in causing dipolar relaxation than are protons, that portion of the relaxation arising from interactions with the exchangeable protons will be greatly reduced in 90% D_2O, but contributions from G-N1 and exchange with the solvent will be unaffected. The results from this experiment are given in Table I. At 20 °C, the semiselective spin–lattice relaxation rate (R_1^{ss}) is reduced from 15 to 1.6 s^{-1} and R_2 is reduced from 106 to 37 s^{-1}. The 10-fold decrease in the spin–lattice relaxation rate suggests that at 20 °C R_1^{ss} is mainly due to magnetic dipolar interactions with the exchangeable guanine and cytosine amino groups. The spin–spin relaxation rate decreases by 70% showing that interaction with G-N1 contributes about 30% of the observed dipolar relaxation.

These results are expected and confirm certain essential features of the theory. Since R_1^s depends mainly on the $J_0(\omega_i - \omega_s)$ spectral densities, only the zero frequency terms arising from proton–proton interactions are expected and found to contribute significantly to R_1^s. The expression for R_2 contains $J_0(0)$ terms in addition to the $J_0(\omega_i - \omega_s)$ terms so the N–H dipolar interaction also contributes a zero frequency term to the spin–spin relaxation. This explains the large value observed for R_2 in 90% D_2O (37 s^{-1}).

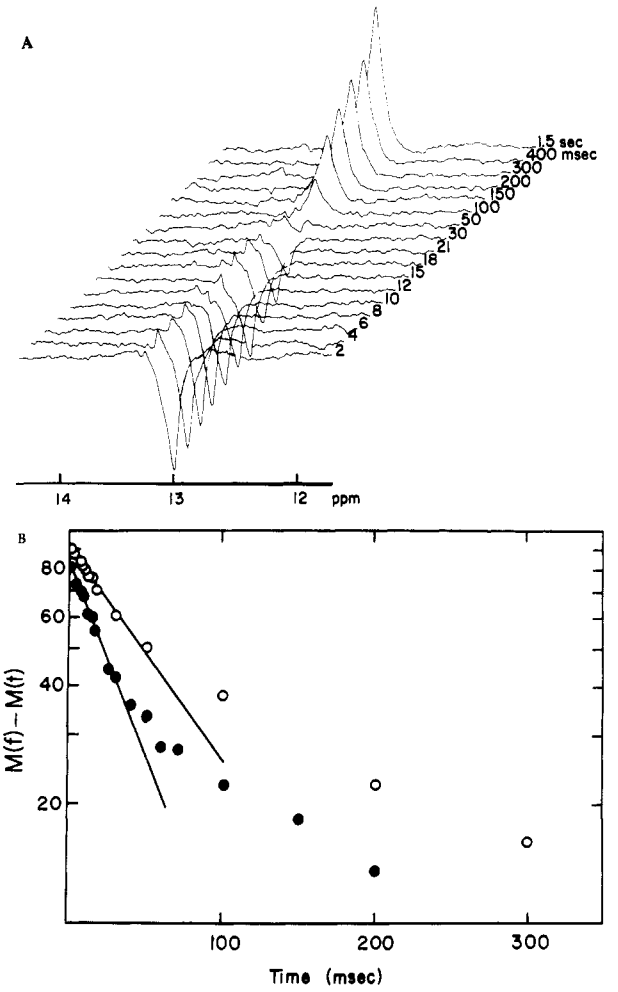

FIGURE 2: (A) Semiselective spin–lattice relaxation measurement, R_1^{ss}, on the imino protons of B-form poly(dG-dC)·poly(dG-dC) at 20 °C. (B) Semilog plot of the recovery of the imino protons in B-form (○) and Z-form (●) poly(dG-dC)·poly(dG-dC) at 20 °C. Note the nonexponential behavior of these recovery curves showing the spin-diffusion dominates spin–lattice relaxation in this system.

Spin Dynamics in Poly(dG-dC)·Poly(dG-dC). Figure 2A shows a semiselective spin–lattice relaxation rate measurement on the hydrogen-bonded imino protons of B-form poly(dG-dC)·poly(dG-dC) at 20 °C. A semilog plot of these data and those obtained for the Z form is shown in Figure 2B. An important feature of Figure 2B is the nonexponential recovery of magnetization for both the B and Z forms. This illustrates that spin–diffusion is important in the spin–lattice relaxation and that the rates are sensitive to the initial preparation of the spin system. The initial relaxation rate, following *selective* excitation of the imino proton, depends on J_0 (see eq 3), but after some time there is an equilibration of the spin-polarization among the five strongly interacting exchangeable protons. The relaxation then depends on J_1 and J_2 (eq 4). Analysis of the experimental data to obtain values of specific rate constants is complicated because, at long times, transfer of magnetization from the five exchangeable protons in a base pair to the 17 nonexchangeable protons [spin–diffusion, characterized by a rate constant R(exch − nonexch)] also contributes to the relaxation of the exchangeable protons (see

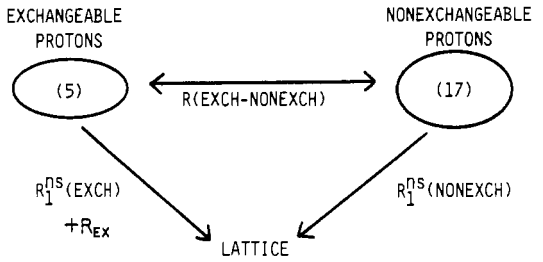

FIGURE 3: Schematic diagram of relaxation pathways for the five exchangeable and 17 nonexchangeable protons (per base pair) in poly(dG-dC)·poly(dG-dC).

Table II: Relaxation Rates Used To Determine R_1^{ns} of Imino Proton in Poly(dG-dC)·Poly(dG-dC)[a]

relaxation rate	rate (s^{-1}) B form	Z form
nonexchangeable protons after nonselective excitation [R_1^{ns}(nonexch)] in D_2O	0.67 ± 0.03	0.36 ± 0.02
imino proton at long times after selective excitation [R_{ex} + R(exch − nonexch) + R_1^{ns}(imino)]	3.6 ± 0.3	4.7 ± 0.6
imino proton after exciting all DNA resonances in H_2O	0.9 ± 0.1	0.8 ± 0.1
calculated imino R_1^{ns}	2.1 ± 0.6	2.4 ± 0.6
calculated spin–diffusion rate connecting the exchangeable and nonexchangeable protons [R(exch − nonexch)]	1.4 ± 0.6	2.3 ± 0.6

[a] See Figure 3.

Table III: Observed Spin–Spin and Spin–Lattice Relaxation Rates of the Various Base Protons of B-Form Poly(dG-dC)·Poly(dG-dC) in 0.1 M NaCl, pH 7, at 20 and 50 °C

rate measured	temp (°C)	rate (s^{-1}) imino	G-H8	C-H6
R_1^{ns}	20	2.1 ± 0.6	0.69 ± 0.09	0.65 ± 0.07
R_2	20	106 ± 10	66 ± 6	88 ± 6
	50	93	46	54
R_1^s	20	23 ± 2	23 ± 2	25 ± 2
	50	23 ± 4	18	15
R_1^{bs}(C-6–C-5)	20			15 ± 4
	50			11
R_2/R_1^s	20	4.6 ± 0.6	2.9 ± 0.4	3.5 ± 0.4
	50	4.0	2.6	3.6 ± 0.5
R_1(C-6–C-5)[a]	20			10 ± 5
	50			4

[a] Contribution to C-H6 relaxation due to interaction with C-H5.

Table IV: Spin–Lattice and Spin–Spin Relaxation Rates in Z-Form Poly(dG-dC)·Poly(dG-dC) at 20 °C[a]

rate measured	rate (s^{-1}) imino	G-H8	C-H6
R_s^{ns}	2.4 ± 0.6	0.36 ± 0.01	0.37 ± 0.02
R_2	162 ± 15	47 ± 5	67 ± 7
R_1^s	32 ± 7	17 ± 2	26 ± 3
R_1^{bs}			14 ± 4
R_2/R_1^s	5 ± 1	2.8 ± 0.1	2.7 ± 0.3
R_1^s(C-H6–C-H5)[b]			12 ± 5

[a] The sample contained 4.5 M NaCl and 0.01 M cacodylate, pH 7. [b] Contribution to C-H6 relaxation due to interaction with C-H5.

Figure 3). If equilibration of magnetization with the 17 spin system occurs, the rate R_1^{ns}(nonexch) (rate at which the collection of 17 nonexchangeable protons separately relax after nonselective excitation) is also involved (see Figure 3). To disentangle these various rate constants, we first directly evaluated R_1^{ns}(nonexch) by performing a nonselective spin–lattice relaxation rate measurement in 100% D_2O (see Table II for rates). A second piece of data is the relaxation rate of the imino proton at long times after selective excitation, which gives R_1^{ns}(exch) + R(exch − nonexch) + R_{ex}. The third and final piece of information is the relaxation rate of the imino proton following a nonselective excitation of *all* protons in the DNA molecule.

The values of R_1^{ns}(imino) and R(exch − nonexch) were obtained by fitting the imino proton relaxation curve resulting from nonselective excitation of all the DNA protons with the kinetic model where the five tightly coupled exchangeable protons interact with the 17 tightly coupled nonexchangeable protons (Figure 3). The value of R_1^{ns}(nonexch) is known, and we required that R_1^{ns} + R(exch − nonexch) for the imino proton was equal to the relaxation rate observed at long times after selective excitation of the imino proton. The exchange of the imino proton with solvent [0.5 s^{-1} (Mirau & Kearns, 1985)] also contributes to the relaxation of the five exchangeable spins in the B form, so the effective contribution to the relaxation of each of the five spins is just $(1/5)R_{ex}$ = 0.1 s^{-1}, and this was subtracted from the value of R_1^{ns} obtained in the kinetic analysis. The final values for R_1^{ns}(imino) and R(exch − nonexch) are given in Table II.

Figure 4 shows pin–lattice relaxation measurements of the nonexchangeable protons of poly(dG-dC)·poly(dG-dC) obtained following different initial preparations of the spin system. Figure 4A shows a relaxation measurement following nonselective excitation of the 17 nonexchangeable protons in D_2O. The relaxation is slow and the same for all the spins. At 20 °C, we find R_1^{ns}(nonexch) ~ 0.7 s^{-1}. Figure 4B shows a relaxation rate measurement where C-H6 has been *selectively* excited by a 180° "soft" pulse from the decoupler. This relaxation rate, R_1^s, is much faster than R_1^{ns}. Like the imino proton relaxation shown in Figure 2B, the recovery of C-H6 is nonexponential (data not shown), and only the initial rates may be interpreted with eq 3. Figure 4C shows a biselective relaxation rate measurement where both C-H6 and C-H5 have been excited. the difference beween the selective and biselective relaxation rates is a measure of the C-H6–C-H5 interaction (see eq 5).

Figure 4D shows a spin–spin relaxation rate measurement on B-form poly(dG-dC)·poly(dG-dC) in D_2O. Table III list various relaxation rates for the imino, G-H8 and C-H6 protons of B-form poly(dG-dC)·poly(dG-dC) at 20 and 50 °C, and Table IV lists the data for Z-form poly(dG-dC)·poly(dG-dC) at 20 °C. These data, along with the ratios R_2/R_1^s, show several interesting features of the proton relaxation in the GC base pair. Theoretically (eq 3 and 7), we expect that in the slow-motion limit R_2/R_1^s = 2.5 for proton dipolar interactions. For G-H8, where measurement of R_2 is uncomplicated by scalar coupling and interaction with like spins is remote, the observed ratio is close to these expected values. The ratio for C-H6 (3.5) in B form is larger than the theoretical maximum.

For imino protons, the ratio of R_2/R_1^s is considerably larger than 2.5 in both B and Z forms because interactions of the imino proton with G-N1 and with the imino protons of neighboring base pairs both contribute to R_2, but not to R_1^s. The contribution of the G_{im}–G_{im} interaction to the observed R_2 can be evaluated as follows (Behling & Kearns, 1985). The theoretically expected contribution of the guanine and cytosine amino protons to the observed R_2 in the B form is $2.5R_1^s$s (=23 s^{-1}) = 57 s^{-1}. The G_{im}–G-N1 contribution of 33 s^{-1} comes from the observed R_2 (=37 s^{-1}) in 90% D_2O less the contribution from residual amino protons (1.6 s^{-1} × 2.5 = 4 s^{-1}). Subtracting the R_2 contributions of the G_{im}–G-N1 and the amino protons from the observed R_2 (=106 s^{-1}) in H_2O gives the R_2 arising from the G_{im}–G_{im} interaction between neighboring identical base pairs as 16 s^{-1}. This factor is large because there

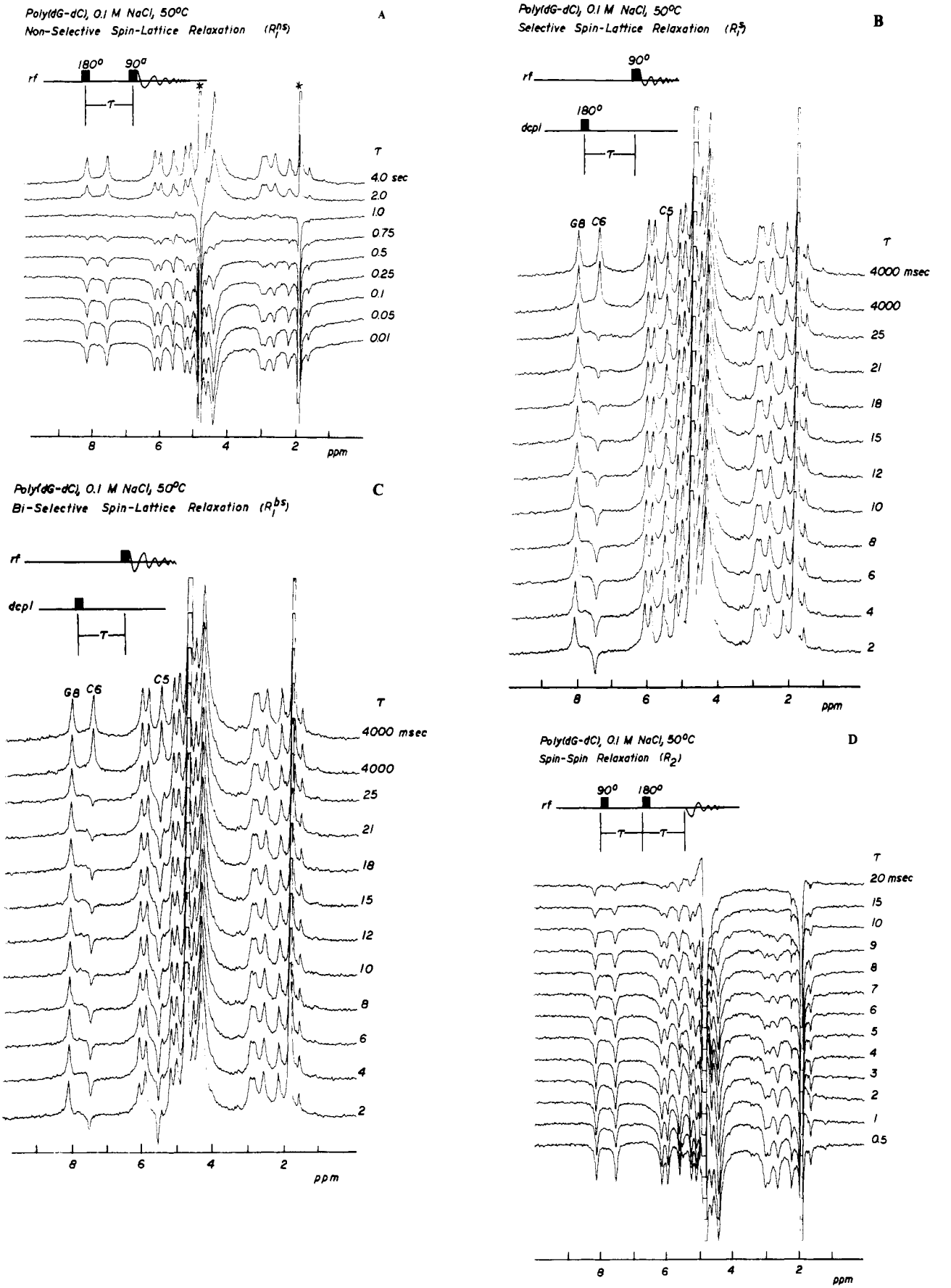

FIGURE 4: (A) Nonselective spin–lattice relaxation measurement (R_1^{ns}) on the nonexchangeable protons in B-form poly(dG-dC)·poly(dG-dC) at 50 °C and 360 MHz in D_2O. Note that in this nonselective experiment all protons have the same relaxation rate. The HOD and the cacodylate peaks are marked (*). (B) Selective spin–lattice relaxation measurement on the C-H6 proton in B-form poly(dG-dC)·poly(dG-dC) at 50 °C and 360 MHz in D_2O. (C) Biselective spin–lattice relaxation measurement (R_1^{bs}) on the C-H6 and C-H5 in B-form poly(dG-dC)·poly(dG-dC) at 50 °C and 360 MHz in D_2O. (D) Spin–spin relaxation measurement (R_2) on the nonexchangeable protons in B-form poly(dG-dC)·poly(dG-dC) at 50 °C and 360 MHz in D_2O.

Table V: Comparison of Effects of Temperature on Relaxation Rates (R) and Line Widths (LW) of the Various Protons in B-Form Poly(dG-dC)·Poly(dG-dC)[a]

proton	LW(20 °C) (Hz)	LW-(calcd)[c]	LW(50 °C)/LW-(20 °C)	R_1^s(50 °C)/R_1^s(20 °C)	R_2(50 °C)/R_2-(20 °C)
imino[b]	65 ± 5	34 ± 3	0.7 ± 0.1	1.0 ± 0.2	0.9 ± 0.2
G-H8	37 ± 5	21 ± 2	0.8 ± 0.2	0.8 ± 0.2	0.7 ± 0.1
C-H6	43 ± 5	28 ± 5	0.6 ± 0.1	0.6 ± 0.1	0.6 ± 0.1

[a] The ratio of (T/η) at 20 and 50 °C is $(T/\eta)_{20}/(T/\eta)_{50} = 0.50$. [b] The imino proton relaxation rates at 50 °C have been corrected for the exchange contribution of 3 s^{-1}. [c] Line width calculated from measured R_2 value (LW = R_2/π).

are two possible neighbors, like spins are 1.8 times more efficient than unlike spins at causing spin–spin relaxation and vertical interactions (along the helix axis) are 3 times more efficient than those in the plane of the bases. Combining these factors, we find that a 16-s^{-1} contribution to R_2 from interactions with imino protons of the neighboring GC base pairs can be accounted for if the vertical separation between imino protons is ~3.7 Å. If the imino protons are located off the helix axis, correspondingly smaller distances would be required.

Effect of Temperature on Relaxation. The effect of temperature on relaxation of the base protons in poly(dG-dC)·poly(dG-dC) illustrates some unusual features that may be common to other DNA. Many nucleic acids undergo conformational changes at temperatures far below that of duplex melting (Palecek, 1969; Gennis & Cantor, 1972; Sarocchi & Guschlbauer, 1973; Brahms et al., 1976; Patel, 1978). If these conformational changes alter interproton distances, they would also affect the relaxation behavior.

(*A*) *Dipolar Relaxation.* Proton relaxation in DNA is expected to be temperature dependent because a large part of the relaxation results from slow tumbling of the helix in solution, and the correlation times for the tumbling of the helix are proportional to the ratio T/η (Diekmann et al., 1982). Table V summarizes the temperature dependence of the dipolar relaxation rates and line widths of the G-H8, C-H6, and imino protons for B-form poly(dG-dC)·poly(dG-dC) at 20 and 50 °C. Over this temperature range, T/η decreases by a factor of 2. Table V shows that while the changes in the relaxation of the C-H6 proton corresponds closely to that expected from the T/η difference between 20 and 50 °C, the relaxation of the imino and G-H8 protons do not. The imino proton in Z DNA deviates even further from predicted behavior; the relaxation rate ((R_1^s) does not change significantly from 20 to 80 °C (see Figure 5) whereas a factor of 3.4 decrease is expected from the change in T/η alone. One possible explanation for this unusual behavior is that the effective interproton distances change as a function of temperature. Since relaxation depends on $\langle r_{is}^{-3}\rangle^2$, shorter internuclear separations are more heavily weighted. Therefore, an increase in the amplitude of motion at higher temperatures could result in a shorter "effective" internuclear separation, and an anomalous temperature behavior may be observed. One-dimensional (1D) and 2D NOE studies show that the G-H2′ proton is primarily responsible for the G-H8 relaxation (Patel et al., 1982; Mirau & Kearns, 1984b), but this distance is sensitive to the relative orientation of the bases and sugar protons. Conversely, the C-H6 relaxation is dominated by the C-H5 proton whose distance is fixed at 2.4 Å. These differences could account for the observation that the C-H6 proton exhibits the expected temperature effect, whereas the G-H8 proton exhibits anomalous behavior.

For the imino protons, there is a temperature-dependent exchange contribution to the spin–lattice relaxation that could, in B DNA, compensate for the variation in T/η over some narrow temperature range. However, this is not the case with Z DNA since exchange in this system is extremely slow (Mirau & Kearns, 1985).

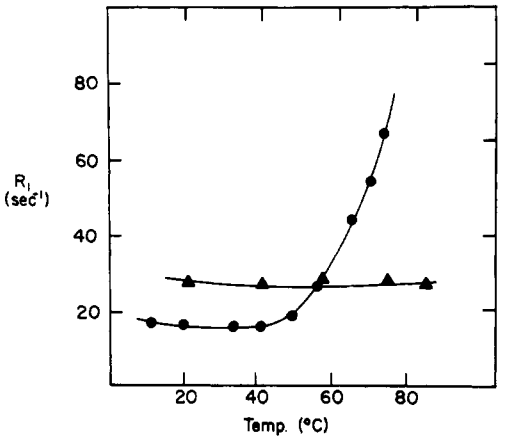

FIGURE 5: Temperature dependence of the imino proton semiselective spin–lattice relaxation rate, R_1^{ss}, in B-form (●) and Z-form (▲) poly(dG-dC)·poly(dG-dC).

It would be desirable to examine separately the viscosity effects on the proton spectra, but this is difficult because agents added to increase the solvent viscosity invariably have protons that obscure the proton spectra or create dynamic range problems. The viscosity can be increased by adding salt to the solution, as was done to convert the DNA to the Z form. This results in an increase (factor of 1.7) in the observed relaxation rate for the imino protons at 20–30 °C.

(*B*) *Effect of Temperature on Imino Proton Exchange.* The imino proton relaxation rates also contain a contribution from proton exchange with solvent protons (Early et al., 1980b, 1981a,b). From previous studies (McConnell, 1978, 1984), it is known that the intrinsic rate of exchange of the imino protons in the free bases is fast and that the slow rate of exchange in the DNA double helix is due to their protection from the solvent (McConnel & Von Hippel, 1970; Teitelbaum & Englander, 1975a,b; Mandal et al., 1979). Their exchange rate is a measure of the fluctuations in DNA structure that expose the imino protons to the solvent.

Figure 5 shows the temperature dependence of the imino proton semiselective spin–lattice relaxation rate (R_1^{ss}) in the B and Z forms of poly(dG-dC)·poly(dG-dC) and illustrates a dramatic difference between B and Z DNA. At low temperatures, where relaxation is due to magnetic dipolar interactions with the guanine and cytosine amino protons, the rates are relatively insensitive to temperature for both B and Z DNA. Above 50 °C, however, the B-form relaxation rate increases rapidly because of exchange, and subtraction of the relatively temperature-independent dipolar contribution to relaxation yields the imino proton exchange rate. For the Z form, however, no such increase in R_1^{ss} is observed with increasing temperature, and we conclude that the exchange rate at 85 °C is insignificant compared to the dipolar relaxation rate (i.e., less than 2 s^{-1}). In real-time exchange experiments (Mirau & Kearns, 1985), we directly measured the imino exchange rate at lower temperatures and find an extrapolated value of ~1 s^{-1} at 85 °C. At this same temperature, exchange from the B form occurs at a rate of 225 s^{-1}. An Arrhenius analysis of the exchange behavior shows that the activation energy for exchange from the B form is 20.4 ± 0.2 kcal/mol. Experiments with poly(rG)·poly(rC) Mirau & Kearns, 1985) and poly(dA-dbr^{5}C)·poly(dG-dT) (unpublished data) shows that the salt concentrations required to induce formation of

Table VI: Proton–Proton and Proton–Nitrogen Distances in a Guanosine–Cytosine Base Pair[a]

interaction	distance (Å)	interaction	distance (Å)
imino–G-NH2	2.2	imino–imino	3.6
imino–C-NH2	2.5	C-H6–C-H5	2.4
imino–G-N1	1.10		

[a] Protons were added to coordinates reported by Taylor & Kennard (1982) and Arnott (personal communication). The listed imino interactions account for ~90% of the relaxation of the imino proton in poly(dG-dC)·poly(dG-dC).

Z DNA do not affect the exchange chemistry, so the difference between exchange in B and Z DNA is a conformational affect on the exchange behavior. These experiments show that the slow conformational fluctuations leading to proton exchange are greatly suppressed in Z DNA compared to B DNA.

(C) Relationship between R_2 and Line Width. Table V illustrates another unusual feature of proton relaxation in DNA molecules previously noted for DNA restriction fragments (Early et al., 1980b) and poly(dA-dT)·(dA-dT) (Assa-Munt et al., 1984), namely, a discrepancy between the measured line width and that calculated from R_2. For example, at 20 °C we calculate an imino proton line width of 34 Hz on the basis of the measured R_2 of 106 s^{-1}, whereas the observed value is 65 Hz. At 20 °C, all the line widths are roughly a factor of 2 greater than those predicted from R_2. The most likely explanation is conformational heterogeneity in the double helix resulting in a variation of ring-current shifts from neighboring bases (chemical shift dispersion). Furthermore, such conformational irregularities must persist for a long time (>10 ms) not to be averaged at room temperature.

Theoretical Calculations of Relaxation Rates. To apply the theoretical expressions for relaxation rates summarized in Appendix A, it is first necessary to specify the relevant interproton distances, and the most important ones are listed in Table VI. In addition to the interproton distances listed here, we included in our calculations other more distant proton–proton interactions (assuming B or Z conformation) but find that their contributions are small (~10%) and insensitive to the precise helical geometry. The second aspect of the calculation requires specification of an appropriate model describing the overall tumbling of the DNA and the internal motions of the bases.

Since the overall tumbling times of the DNA molecules vary with the length of the molecule, the theoretical analysis of the relaxation rates could be complicated because our samples are not monodisperse. In a previous study of sonicated poly(dA-dT)·poly(dA-dT) (average size ~50 base pairs), we examined the effect of heterogeneity in the size distribution on the NMR relaxation properties (Assa-Munt et al., 1984). We found that the behavior predicted for the experimentally determined distribution of molecular lengths was identical with that predicted for a monodisperse sample with a length equal to the average size in the heterogeneous sample. Since dispersion of molecular lengths is virtually the same in poly(dG-dC)·poly(dG-dC) and poly(dA-dT)·poly(dA-dT), we conclude that the same holds true for poly(dG-dC)·poly(dG-dC). Thus, we do not think that our results are being measurably affected by the molecules that are of higher or lower weight than the average-sized molecule and that it is proper to analyze the relaxation rates by using the average molecular size.

To extract information about internal motions in the DNA from relaxation rates, we examined a variety of different models to identify the types of internal motion that must be introduced to obtain agreement between experiment and theory. The expressions derived by Woessner and by Whittebort and Szabo (Woessner, 1962; Woessner et al., 1969; Wittebort & Szabo, (1978) are used to calculate relaxation rates for the various models, and these results are summarized in Tables VII and VIII. The significant features of the different models are discussed below.

(A) Rigid-Rod Model. The simplest model treats the DNA as a 60 base pair rigid rod. This model reasonably accounts for the overall tumbling of the molecule since the persistence

Table VII: Comparison of the Imino and C-H6–C-H5 Relaxation Rates for the B Forms of Poly(dG-dC)·Poly(dG-dC) Observed at 20 °C with the Values Calculated Using Various Motional Models[a]

model	imino			C-H6
	R_1^s (s^{-1})	R_2 (s^{-1})	R_1^{ns} (s^{-1})	R_1(C-H5–C-H6) (s^{-1})
observed value [B form (0.1 M NaCl)]	23 ± 1	106 ± 10	2.1 ± 0.6	10 ± 5
calculated for 60-bp rigid rod, τ_1 = 242 ns, τ_a = 15.8 ns	66	296	0.12	29
calculated for 60-bp rigid rod, τ_1 = 242 ns, τ_a = 6 ns	54	253	0.3	21
calculated for 35-bp rigid rod, τ_1 = 69 ns, τ_a = 8.8 ns	24	103	0.23	8
calculated for 60-bp rigid rod with three-site jump, $\Delta\theta$ = ± 32°, τ_i = 1.0 ns, τ_1 = 242 ns, τ_2 = 15.8 ns	24	103	2.3	8
calculated for 60-bp rigid rod with three-site jump, $\Delta\theta$ = ±29°, τ_i = 1 ns, τ_1 = 242 ns, τ_a = 6 ns	24	110	2.1	9
calculated for 60-bp rigid rod with longitudinal and azimuthal jumps and torsion, τ_1 = 242 ns, τ_a = 6 ns, τ_{1ng} = 100 ns, $\Delta\theta$ = 35°, τ_{az} = 0.25 ns, $\Delta\phi$ = 40°	22	105	2.4	7

Table VIII: Comparison of the Imino and C-H6–C-H5 Relaxation Rates for the Z Forms of Poly(dG-dC)·Poly(dG-dC) Observed at 20 °C with the Values Calculated Using Various Motional Models[a]

model	imino			C-H6
	R_1^s (s^{-1})	R_2 (s^{-1})	R_1^{ns} (s^{-1})	R_1(C-H5–C-H6) (s^{-1})
observed value [Z form (4.5 M NaCl)]	32 ± 7	162 ± 15	2.4 ± 0.6	12 ± 5
calculated for 60-bp rigid rod, τ_1 = 642 ns, τ_a = 28.5 ns	159	722	0.06	60
calculated for 60-bp rigid rod, τ_1 = 642 ns, τ_a = 6 ns	130	617	0.30	51
calculated for 30-bp rigid rod, τ_1 = 122 ns, τ_a = 13.5 ns	40	172	0.15	14
calculated for 60-bp rigid rod with three-site jump, $\Delta\theta$ = 37°, τ_i = 1.0 ns, τ_1 = 642 ns, τ_a = 28.5 ns	35	155	2.6	13
calculated for 60-bp rigid rod with three-jump, $\Delta\theta$ = 35°, τ_i = 1.0 ns, τ_1 = 642 ns, τ_a = 6 ns	35	163	2.6	11
calculated for 60-bp rigid rod with longitudinal jump and azimuthal jump and torsion, τ_1 = 642, τ_a = 6 ns, τ_{1ng} = 100 ns, $\Delta\theta$ = 39°, τ_{az} = 0.25 ns, $\Delta\theta$ = 40°	29	162	2.3	8

length of poly(dG-dC)·poly(dG-dC) is ~250 base pairs (Thomas & Bloomfield, 1983), but it does not allow for any internal motion. In the rigid-rod model, relaxation rates depend only on the tumbling rates of the DNA helix about the long and short helix areas and the magnitude and orientation of internuclear vectors relative to the long axis of the helix (Woessner, 1962). The tumbling rates may be calculated from the helix length with the Tirado and Garcia de la Torre formula (Tirado & Garcia de la Torre, 1980; Elias & Eden, 1981). For B-form poly(dG-dC)·poly(dG-dC), the rise per residue is 3.4 Å, and the helix diameter is 26 Å (Dickerson & Drew, 1981), while for Z-form DNA these values are 3.7 and 22 Å (Wu et al., 1981). The viscosity of the DNA solutions at 20 °C was assumed to be 1 cP and for the Z form, in 4.5 M NaCl solution, 2.2 cP. The relaxation rates calculated from these data are given in Tables VII and VIII.

(*B*) "*Torsionally Flexible Rod*". To mimic the effects of torsional motion of the DNA detected by fluorescence polarization anisotropy measurements (Barkely & Zimm, 1979; Millar et al., 1981; Magde et al., 1983; Thomas & Schurr, 1983; Ashikawa et al., 1984), we have used a model in which the end over end tumbling of the DNA is still characterized by a correlation time characteristic of a 60 base pair rod (i.e., 242 ns), but the correlation time for axial spinning is reduced from 16 to 6 ns. This results in only small decreases in the magnitudes of those relaxation rates that depend on $J_0(0)$ (the selective spin–lattice relaxation rates and the spin–spin relaxation rates) but *increases* the nonselective relaxation rates that depend on $J_1(\omega)$ and $J_2(\omega)$ (see Table VII).

(*C*) "*Rod with Bending*". To simulate bending motions of the DNA (or internal motions of the bases relative to the helix axis), without introducing torsional motions, we simply reduced the "effective" size of the DNA from 60 to 35 base pairs, as in a previous study (Early & Kearns, 1979; Early et al., 1980a). This reduction in effective size diminishes the correlation time for end over end tumbling (from 242 to 69 ns) and causes a 3-fold reduction in all relaxation rates that depend primarily on the value of $J_0(0)$ (R_1^s and R_2). Comparison of these results with those obtained for the torsionally flexible rod immediately reveals that R_1^s and R_2 are much more sensitive to out of plane motions of the bases than to torsional motions. Although this model yield R_1^s and R_2 values that agree with the experimental values for both B and Z DNA, the predicted nonselective rates are too small because of the absence of fast internal motions.

(*D*) *DNA with Local Motions* (*Base-Pair Wobble*). In this model, the correlation times for end over end tumbling and for axial spinning of the DNA are taken to be those appropriate for a rigid 60 base pair DNA, but a three-site jump on the surface of a cone model was used to mimic the effects of restricted out of plane wobble of the bases (Woessner, 1962). With this model, we find agreement between all experimental and calculated relaxation rates when amplitudes of about ±30° and a correlation time of 1 ns are used. An internal motion correlation time of 4×10^{-11} s would give an equally good fit of the data but is rejected as physically unreasonable.

(*E*) *Torsionally Flexible Rod with Base-Pair Wobble*. In this model, the correlation time for end over end tumbling is taken to be 242 ns (rigid-rod value), the axial spinning correlation time is reduced to 6 ns to stimulate large-scale collective torsional motions of the DNA that are known to be fast, and a three-site jump on a cone model is added to allow torsional and out of plane local motion (wobble) of the bases. In this case, the correlation time for wobble remains at 1 ns, but there is a small reduction in the amplitude of wobble needed to obtain agreement between experiment and theory.

(*F*) *Torsionally Flexible Rod with Decoupled Longitudinal and Azimuthal Local Motions*. In this final model, the end over end tumbling rate is that of the 60 base pair rigid rod, and cooperative torsional motions are incorporated by setting the axial spinning time to 6 ns. Internal motion is modeled by independent longitudinal and azimuthal three-site jumps with time constants τ_{lng} and τ_{az} and amplitudes $\Delta\theta$ and $\Delta\phi$, respectively (Wittebort & Szabo, 1978). By using two independent jumps, it is possible to separately determine the out of plane and in-plane motions of the bases required to fit the observed relaxation rates. To fit the data, the amplitude of the longitudinal (out of plane) motion must be at least 25° for the B DNA and 32° for Z DNA and is generally in the 30–40° range, depending of τ_{lng}. The longitudinal time constant can range from 1 ns up to ~100 ns. If τ_{lng} values longer than 100 ns are used, much larger out of plane amplitudes are required. The azimuthal jump amplitude, $\Delta\phi$, must be 30–90° and τ_{az} in the range 0.1–1.5 ns to account for the observed relaxation rates.

Discussion

The internal dynamics of the B and Z forms of poly(dG-dC)·poly(dG-dC) were examined by proton relaxation rates. With two-dimensional NMR (Mirau & Kearns, 1984b), solvent substitution, and several excitation schemes, we first established the major relaxation pathways for the various protons in poly(dG-dC)·poly(dG-dC) and found that the spin–lattice relaxation of the imino protons is dominated by interactions with the nearby exchangeable amino protons of guanine and cytosine. These same interactions also dominate the spin–spin relaxation of the G-N1, but about 30% of the observed rate is due to the nitrogen–proton interaction with G-N1.

Internal Motion in B and Z DNA. The measured proton relaxation rates provide information about fluctuations in DNA structure that occur in the nanosecond to microsecond time range. By comparing the observed relaxation rates with those calculated from different models for the internal and overall motions of the DNA, we are able to identify the types of motions that must be present and establish their amplitudes and correlation times. A comparison of experimental and theoretical relaxation rates (Tables VII and VIII) reveals the striking feature that the R_1^s and R_2 rates calculated for a rigid-rod model of DNA are about 3 times faster than the observed rates in B DNA and 5 times faster for Z-form DNA. The discrepancy would be even larger if the molecules are tumbling more slowly than we estimate due to intermolecular association in the NMR samples. These large discrepancies between the rigid-rod theory and experiment indicate that the DNA does not behave as a rigid rod. Reducing the correlation time for spinning the helix axis to 6 ns to account for collective torsional motions is ineffective in reducing the calculated values of R_1^s or R_2, but a reduction in the correlation time for end over end tumbling time to 69 ns is effective. From this we conclude that bending of the DNA and out of plane motions of the bases relative to the helix axis are important. However, because this model does not account for the observed value of R_1^{ns}, there must be some additional high-frequency motions present. A good fit of all the relaxation rates can be obtained with a model that allows for fast azimuthal motions of the bases (0.1–1.5-ns correlation time and ±30° amplitude) and slower (1–100 ns), large-amplitude (±30°) out of plane motions of the bases relative to the helix axis in addition to fast, collective torsional motions of the helix (modeled by 6-ns axial spinning of the helix). A good fit is also obtained with

a three-site jump on the surface of a cone model that allows for ±30° motions of the base with a correlation time of ~1.0 ns for both B and Z DNAs.

Since several models could fit the experimental rates, it is important to note those features that must be present in all models. The first point demonstrated by the results shown in Tables VII and VIII is that torsional motions alone are incapable of bringing the calculated rates for R_1^s and R_2 into agreement with experiment. Only by allowing for large-amplitude (~±30°), out of plane motions of the bases do we obtain agreement with experiment. The second point is that the required amplitude of the out of plane motion is set by the magnitudes of R_1^s and R_2, but it is difficult to rigorously establish the correlation time for such motions because the data can be fit with various combinations of correlation times for torsional and out of plane motions. We know, however, that the out of plane correlation time must be shorter than ~100 ns to get reasonable values for the out of plane amplitude. This upper limit for the correlation time is established because the out of plane motions must be fast compared with the overall tumbling of the molecule to affect the relaxation rates. Since discrepanices between the observed rates and those calculated with a rigid-rod model persist even in shorter DNA (Early et al., 1980b, 1981b), we believe that the wobble correlation times are even shorter than the upper limits reported here. The third point is that collective torsional motions alone are insufficient to fit the R_1^{ns}, and there must be fast (0.1–1.5-ns), large-amplitude (±30–40° local torsional motions present in the bases.

Comparison of B and Z DNAs. The analysis of the Z-DNA relaxation rates is analogous to that used in analyzing the B-DNA data and produces similar results for the motional amplitudes and time constants. In particular, large-amplitudes out of plane motions (±35°) are required, although the correlation time may be longer than that needed to fit the B-DNA data. As in B-DNA, we also require rapid local torsional motions in addition to collective torsional motions of the bases to fit the nonselective relaxation rates. Since light scattering experiments indicate that the persistence length of the Z form is 200 nm as compared with 84 nm for the B form of poly(dG-dC)·poly(dG-dC) and 61 nm for calf thymus DNA (Thomas & Bloomfield, 1983), we anticipated a difference in the relaxation behavior of B and Z DNA. Our measurements indicate that while there is some reduction in the amplitude or increase in the correlation time of the high-frequency sugar motions in Z DNA, the motions of the bases are similar in B and Z DNA. These results are to be contrasted with the recent fluorescence polarization results of Ashikawa et al. (1984) that indicate the Z form is *more flexible* than the B-form DNA (both in torsion and bending) by factors of 4–6.

Relation to Previous Studies of Internal Motion in DNA. The above analysis shows that both B and Z forms of poly(dG-dC) exhibit large-amplitude (±35°) out of plane motions of the bases (correlation times <70–100 ns) and fast torsional motions of the bases and sugar groups. Previous NMR measurements (Bolton & James, 1979; Early & Kearns, 1979; Hogan & Jardetzky, 1980; Levy et al., 1981; Keepers & James, 1982) indicate there are substantial motions in the backbone of native DNA, but there has been little analysis of the base motion. In an earlier study of motion in poly(dA-dT)·poly(dA-dT), we found similar results for amplitudes of base motion and the presence of fast motions. One modification of our earlier conclusions, now required in light of the present analysis, is that the correlation time for out of plane motion may be longer than the lower limit of 2.5 ns we initially estimated. The original analysis used a three-site jump on the surface of a cone model to simulate *both* out of plane and torsional motions of the bases, and a single correlation time was associated with that motion. In the present analysis we have uncoupled these two motions and find that a considerably longer correlation time is permitted for the out of plane motion, but the local torsional motions are still required to be fast.

Several different theoretical models have been developed to describe the elastic deformations of DNA and the fluorescence depolarization that arises from these motions. In the Barkely–Zimm model (Barkely & Zimm, 1979), the torsional motions account for most of the depolarization although they noted that the measurements are not sensitive to bending motions when the dye transitions are oriented perpendicular to the helix axis. Shibata (unpublished results) recently analyzed fluorescence polarization anisotropy (FPA) as well as transient photodichroism (TPD) measurements and again found that most of the observed depolarization can be accounted for by torsional motions. We have recently carried out steady-state FPA measurements in which two differently polarized dye transitions were excited, and we too found that the correlation time for out of plane motions of the dye (and presumably the bases) is much longer than for torsional motions (T. Härd and D. R. Kearns, unpublished results).

Although the NMR results generally agree with the FPA measurements, there are certain differences. First, fast motions (in the 1–2-ns range) seem to be required by the NMR, but these motions may in part be related to the motions leading to the initial rapid depolarization of the ethidium fluorescence. Second, the out of plane motions required to account for the NMR measurements appear to be larger than those inferred by the fluorescence measurements and to have a smaller correlation time.

There are several possible reasons why the amplitudes of out of plane motion deduced from NMR are larger than those derived from measurements on fluorescence probes. One possibility is that we incorrectly evaluated the amplitude of the internal motion of the bases by using incorrect rotational correlation times for the DNA. In the present calculations, we assume rigid-rod rotational behavior of the DNA that is appropriate for dilute solutions. However, rotation is likely to be even slower at NMR concentrations, and we have FPA evidence that this is the case (T. Härd and D. R. Kearns, unpublished results). Slower tumbling would require even larger out of plane motions than determined here. Another possibility is that the intercalated fluorescent probe (usually ethidium bromide) suppresses some of the high-frequency motions of the bases it presumably monitors. That intercalating drugs exhibit excluded site binding (Crothers, 1968; Bauer & Vinograd, 1970; Sobell et al., 1976) certainly indicates that there is a perturbation of the local structure of the DNA at the drug binding site. Moreover, an intercalated chromophore that stacks with bases on both strands may not be able to monitor propellering motions that would be detected by NMR. The chromophore could, however, follow cooperative rolling and tilting motions of neighboring base pairs.

It is interesting that the bases in poly(dA-dT)·poly(dA-dT) experience fluctuations of similar amplitude and frequency (Assa-Munt et al., 1984) as those reported here for the B and Z forms of poly(dG-dC)·poly(dG-dC). Thus, there appears to be little sequence dependence of these nanosecond internal motions in synthetic DNA. Finally, we point out that a recent analysis of the X-ray diffraction data for the DNA duplex d(CGCGAATTCGCG) indicates that even in the crystalline state the DNA bases may undergo large (±15°) librations and the sugar groups exhibit even larger amplitude motions

(Holbrook & Kim, 1984). If the amplitudes of the base and sugar motions are larger in the crystal, we expect even more motion in solution. The detection of large-amplitude, rapid internal motions of the bases and the backbone of DNA in solution raise interesting questions about the role that subtle sequence-dependent variations in conformation might play in protein–DNA interactions. While our experiments are not able to distinguish between cooperative and uncorrelated motions of the bases, the amplitudes are sufficiently large that one might expect the DNA locally to explore many different conformational states in a short period of time (nanosecond). If true, this would certainly diminish the importance of specific conformational states in the recognition process.

Exchange Rates in B and Z DNAs. In addition to providing information about high-frequency internal motions in DNA, we have also obtained information about these slow conformational fluctuations that result in proton exchange. The conversion from the B to the Z form dramatically alters the rate of exchange of the imino protons (Pilet & Leng, 1982). For B-form poly(dG-dC)·poly(dG-dC) at high temperature, proton exchange with solvent is rapid with an activation energy of 20.1 kcal/m. By contrast, exchange from the Z form is too slow ($<2\ s^{-1}$) to contribute to the NMR relaxation even at temperatures as high as 85 °C. Studies on other DNA and RNA polymers have shown high salt does not affect exchange rates in other DNAs and RNAs (McConnell, 1978, 1984), indicating that the reduced exchange from Z DNA is due to a conformational rather than solvent effect on the exchange. The amino protons of Z-form poly(dG-dC)·poly(dG-dC) and poly(dI-dbr^{5}C) also exchange slowly with the solvent (Hartman et al., 1982; Pilet & Leng, 1982), and our NMR studies on other Z-form duplexes (unpublished results) show that the slow exchange is a feature common to Z DNA.

ACKNOWLEDGMENTS

We thank Dr. N. Assa-Munt for assistance in determining the DNA length.

APPENDIX

Theory

Relaxation may occur by several different processes, including proton–proton and proton–nitrogen magnetic dipolar interactions and exchange of the imino protons with the unpolarized solvent protons. The relaxation of protons in DNA has previously been discussed (Assa-Munt et al., 1984) and will be briefly summarized here.

(*A*) *Spin–Lattice Relaxation: Dipolar Contribution.* For two protons, the spin–lattice relaxation of spin i due to magnetic dipolar interactions with spin s is given by (Abragam, 1978)

$$dm_i/dt = -Km_i[J_0(\omega_i - \omega_s) \times (1 - m_s/m_i) + 3J_1(\omega_i) + 6J_2(\omega_i + \omega_s)(1 + m_s/m_i)] \quad (1)$$

where m_i and m_s represent the difference in the longitudinal magnetization of the spin at time t and at thermal equilibrium [i.e., $m_i = (M^i_{zt} - M^i_{zo})/M^i_{zo}$]. The other terms are

$$K = (2/3)\gamma_i^2\gamma_s^2\hbar^2S(S + 1)r_{is}^{-6} \quad (2)$$

where γ_i and γ_s are the gyromagnetic ratios for spins i and s, $\hbar$ is Planck's constant over 2π, r_{is} is the internuclear separation, ω_i and ω_s are the Larmor frequencies, and $J_n(\omega)$, where $n = 0, 1, 2$, are the spectral densities.[1] For the large (60 base pair) DNA molecules studied here, $J_0 \gg J_1, J_2$.

Because the ratio m_s/m_i depends on the initial preparation of the spin system and varies with time, the relaxation behavior may be nonexponential. Several different experimental situations are interesting.

(*i*) *Selective and Nonselective Excitation.* If spin i is selectively excited, then $m_i \neq 0$, $m_s = 0$, and the *initial* relaxation rate, R^s_1, is given by

$$dm_i/dt = -KJ_0(\omega_i - \omega_s)m_i = -R^s_1m_i \quad (3)$$

As relaxation proceeds, m_s increases as m_i decreases, and the decrease of $1 - m_s/m_i$ in eq 1 causes slower (nonexponential) relaxation. When the populations of i and s have been equalized

$$dm_i/dt = -K[3J_1(\omega) + 12J_2(\omega_i + \omega_s)]m_i = -R^{ns}_1m_i \quad (4)$$

This is also the relaxation rate expected after nonselective excitation of both the i and s spins, and under these conditions, the relaxation contains no contribution from the J_0 processes that were responsible for the initial rapid relaxation.

(*ii*) *Semiselective Excitation.* With some excitation pulses (e.g., the time-shared Redfield pulses), both spins i and s are excited, but to different degrees. The initial relaxation rate, R^{ss}_1, of the i spins is decreased compared to R^s_1 by the fact $1 - m_s/m_i$, and the observed rate more quickly approaches the nonselective relaxation rate. This effect is important when the time-shared Redfield 214 pulse (Wright et al., 1981) is used to measure the guanine imino proton relaxation rate since the G and C amino protons are also excited to some extent. The above equations for a pair of interacting spins may be generalized to a multispin system by summing over all the interactions (Kalk & Berendsen, 1976).

(*iii*) *Biselective Excitation.* To extract information about the interaction of any pair of protons in a multispin system, a biselective excitation of the spin system (Broido & Kearns, 1982) may be used. For example, the C-H6 proton interacts with the C-H5 and various sugar protons, resulting in an observed relaxation rate

$$R^s_1(\text{C-H6}) = R^s_1(\text{C-H6–C-H5}) + R^s_1(\text{C-H6–other}) \quad (5)$$

If both C-H5 and C-H6 are excited, they cannot efficiently relax one another (via J_0 processes), so the initial relaxation is almost exclusively from interactions with other protons, i.e., R^s_1(C-H6–other). The difference between the selective and biselective (R^{bs}_1) relaxation rates is the relaxation due to the C-H6–C-H5 interaction. Since the C-H5–C-H6 internuclear separation is 2.4 Å, the magnitude of the spectral density J_0 associated with base motions may be obtained directly from eq 3 (assuming $J_0 \gg J_1, J_2$).

(*B*) *Spin–Spin Relaxation.* Nonselective pulses may be used to measure the spin–spin relaxation rate, R_2, because it does not depend on the initial preparation of the spin system (neglecting J-coupling effects). The transverse relaxation rate for like spins (i.e., $\Delta\nu_{is} = \nu_i - \nu_s \leq R_2/\pi$) and for unlike spins is given by (Abragam, 1978) the following:

for like spins

$$R^l_2 = \frac{\gamma_i^4\hbar^2}{r^6}I(I + 1)[3J_0(0) + 5J_1(\omega_i) + 2J_2(2\omega_i)] \quad (6)$$

for unlike spins

$$R^u_2 = \frac{\gamma_i^2\gamma_s^2\hbar^2}{3r^6}S(S + 1) \times [4J_0(0) + J_0(\omega_i - \omega_s) + 3J_1(\omega_i) + 6J_1(\omega_s) + 6J_2(\omega_i + \omega_s)] \quad (7)$$

[1] For an isotropic rotor $J_n(\omega) = (\tau_c/5)[1 + (\omega\tau_c)^2]^{-1}$.

The expressions for R_2 contain $J_0(0)$ terms in addition to the $J_0(\omega_i - \omega_s)$ terms found in the R_1^s expression. Therefore, proton–nitrogen interactions contribute to R_2 but not to R_1^s. Moreover, since the relaxation is independent of spin populations, imino protons may relax neighboring imino protons (like spins). For reference, a summary of the different relaxation rates discussed above is given under Glossary of Rate Constants.

Glossary of Rate Constants

R_1^s spin–lattice relaxation rate measured at short times after *selective* excitation of a particular resonance; this is the rate a spin loses magnetization via zero-quantum processes

R_1^{ns} rate at which a collection of strongly interacting spins (e.g., the five exchangeable protons or the 17 nonexchangeable protons) collectively relax following their nonselective excitation; this rate does not contain contributions from zero-quantum transitions

R_1^{ss} spin–lattice relaxation rate measured at short times after a partially selective excitation where several spins are excited, but to different degrees; $R_1^{ns} < R_1^{ss} < R_1^s$

R_1^{bs} initial spin–lattice relaxation rate measured after equally exciting two spins in a multispin system; the difference between R_1^{bs} and R_1^s provides information about the zero-quantum relaxation rate

R_2^l, R_2^u spin–spin relaxation rates arising from interactions between spins that resonate at the same or different frequencies, respectively

Registry No. Poly(dG-dC), 36786-90-0.

REFERENCES

Abragam, A. (1978) in *The Principles of Nuclear Magnetism* (Marshall, W. C., & Wilkinson, D. H., Eds.) Chapter 8, Oxford University Press, Oxford, England.

Ashikawa, I., Kinosita, K., & Ikegami, A. (1984) *Biochim. Biophys. Acta 782*, 87–93.

Assa-Munt, N., & Kearns, D. R. (1984) *Biochemistry 23*, 791–796.

Assa-Munt, N., Granot, J., Behling, R. W., & Kearns, D. R. (1984) *Biochemistry 23*, 944–955.

Barkely, M. D., & Zimm, B. H. (1979) *J. Chem. Phys. 70*, 2991–3007.

Bauer, W., & Vinograd, J. (1970) *J. Mol. Biol. 47*, 419–435.

Behling, R. W., & Kearns, D. R. (1985) *Biopolymers 24*, 1157–1167.

Bolton, P. H., & James, T. L. (1979) *J. Phys. Chem. 83*, 3359–3366.

Brahms, S., Brahms, J., & Van Holde, K. E. (1976) *Proc. Natl. Acad. Sci. U.S.A. 73*, 3453–3457.

Broido, M. S., & Kearns, D. R. (1982) *J. Am. Chem. Soc. 104*, 5207–5216.

Crothers, D. M. (1968) *Biopolymers 6*, 575–584.

Dhingra, M. M., Sarma, M. H., Gupta, G., & Sarma, R. H. (1983) *J. Biomol. Struct. Dyn. 1*, 417–428.

Dickerson, R. E. (1983) in *Nucleic Acids: The Vectors of Life* (Pullman, B., & Jortner, J., Eds.) pp 1–15, D. Reidel, Dordrecht, Holland.

Dickerson, R. E., & Drew, H. R. (1981) *J. Mol. Biol. 149*, 761–786.

Diekmann, S., Hillen, W., Morgeneyer, B., Wells, R. D., & Porschke, D. (1982) *Biophys. Chem. 15*, 263–270.

Drew, H., Takano, T., Takana, S., Itakura, K., & Dickerson, R. E. (1980) *Nature (London) 286*, 567–573.

Early, T. A., & Kearns, D. R. (1979) *Proc. Natl. Acad. Sci. U.S.A. 76*, 4165–4169.

Early, T. A., Feigon, J., & Kearns, D. R. (1980a) *J. Magn. Reson. 41*, 343–348.

Early, T. A., Kearns, D. R., Hillen, W., & Wells, R. D. (1980b) *Nucleic Acids Res. 8*, 5795–5812.

Early, T. A., Kearns, D. R., Hillen, W., & Wells, R. D. (1981a) *Biochemistry 20*, 3756–3764.

Early, T. A., Kearns, D. R., Hillen, W., & Wells, R. D. (1981b) *Biochemistry 20*, 3764–3769.

Elias, J. G., & Eden, D. (1981) *Biopolymers 20*, 2369–2380.

Feigon, J., Wright, J. M., Leupin, W., Denny, W. A., & Kearns, D. R. (1982) *J. Am. Chem. Soc. 104*, 5540–5541.

Feigon, J., Denny, W. A., Leupin, W., & Kearns, D. R. (1983a) *Biochemistry 22*, 5930–5942.

Feigon, J., Leupin, W., Denny, W. A., & Kearns, D. R. (1983b) *Biochemistry 22*, 5943–5951.

Gennis, R. B., & Cantor, C. R. (1972) *Biochemistry 11*, 2509.

Granot, J., Assa-Munt, N., & Kearns, D. R. (1982) *Biopolymers 21*, 873–883.

Haasnoot, C. A. G., Westerink, H. P., Van der Marel, G. A., & Van Boom, J. H. (1983) *J. Biomol. Struct. Dyn. 1*, 131–149.

Hartman, B., Pilet, J., Ptak, M., Ramstein, J., Malfoy, B., & Leng, M. (1982) *Nucleic Acids Res. 10*, 3261–3279.

Hill, R. J., & Stollar, B. D. (1983) *Nature (London) 305*, 338–340.

Hogan, M. E., & Jardetzky, O. (1980) *Biochemistry 19*, 3460–3468.

Holbrook, S. R., & Kim, S-H. (1984) *J. Mol. Biol. 173*, 361–388.

Izatt, R. M., Christensen, J. J., & Kytting, J. H. (1971) *Chem. Rev. 71*, 439–480.

Kalk, A., & Berendsen, H. J. C. (1976) *J. Magn. Reson. 24*, 343–366.

Kearns, D. R., Assa-Munt, N., Behling, R. W., Early, T. A., Feigon, J., Granot, J., Hillen, W., & Wells, R. D. (1981) in *Biomolecular Stereodynamics* (Sarma, R. H., Ed.) Vol. I, pp 345–365, Adenine Press, New York.

Keepers, J. W., & James, T. L. (1982) *J. Am. Chem. Soc. 104*, 929–939.

Keepers, J. W., & James, T. L. (1984) *J. Magn. Reson. 57*, 404–426.

Lafer, E. M., Moller, A., Nordheim, A., Stollar, B. D., & Rich, A. (1981) *Proc. Natl. Acad. Sci. U.S.A. 78*, 3546–3550.

Levy, G. C., Hilliard, P. R., Levy, L. F., & Rill, R. L. (1981) *J. Biol. Chem. 256*, 9986–9989.

Lown, J. W., Gunn, B. C., Chang, R. Y., Majumdar, K. C., & Lee, J. S. (1978) *Can. J. Biochem. 56*, 1006–1015.

Magde, D., Zappala, M., Knox, W. H., & Nordlund, T. M. (1983) *J. Phys. Chem. 87*, 3286–3288.

Mandal, C., Kallenbach, N. R., & Englander, S. W. (1979) *J. Mol. Biol. 135*, 391–411.

Matsuoka, Y., & Yamaoak, K. (1979) *Bull. Chem. Soc. Jpn. 52*, 3163–3170.

Matsuoka, Y., & Yamaoka, K. (1980) *Bull. Chem. Soc. Jpn. 53*, 2146–2151.

McConnell, B. (1978) *Biochemistry 17*, 3168–3175.

McConnell, B. (1984) *J. Biomol. Struct. Dyn. 1*, 1407–1421.

McConnell, B., & Von Hippel, P. (1970) *J. Mol. Biol. 50*, 317–332.

Millar, D. P., Robbins, R. J., & Zewail, A. H. (1981) *J. Chem. Phys. 75*, 3648–3659.

Mirau, P. A., & Kearns, D. R. (1983) in *Structure and Dynamics: Nucleic Acids and Proteins* (Clementi, E., &

Sarma, R. H., Eds.) p 227, Adenine Press, New York.
Mirau, P. A., & Kearns, D. R. (1984a) *J. Mol. Biol. 177*, 207–227.
Mirau, P. A., & Kearns, D. R. (1984b) *Biochemistry 23*, 5439–5446.
Mirau, P. A., & Kearns, D. R. (1985) *Proc. Natl. Acad. Sci. U.S.A. 82*, 1594–1598.
Nordheim, A., Lafer, E. M., Peck, L. J., Wang, J. C., Stollar, D., & Rich, A. (1982) *Cell (Cambridge, Mass.) 31*, 309–318.
Palecek, E. (1969) *Prog. Nucleic Acid Res. Mol. Biol. 9*, 31–74.
Patel, D. J. (1978) *J. Polym. Sci. 62*, 117–141.
Patel, D. J., Canuel, L., & Pohl, F. (1979) *Proc. Natl. Acad. Sci. U.S.A. 76*, 2508–2511.
Patel, D. J., Kozlowski, S. A., Nordheim, A., & Rich, A. (1982) *Proc. Natl. Acad. Sci. U.S.A. 79*, 1413–1417.
Pilet, J., & Leng, M. (1982) *Proc. Natl. Acad. Sci. U.S.A. 79*, 26–30.
Pohl, F. M., & Jovin, T. M. (1972) *J. Mol. Biol. 67*, 375–396.
Rich, A., Nordheim, A., & Wang, H.-J. (1984) *Annu. Rev. Biochem. 53*, 791–846.
Robinson, B. H., Lerman, L. S., Beth, A. H., Frisch, H. L., Dalton, L. R., & Auer, C. (1980) *J. Mol. Biol. 139*, 19–44.
Sarocchi, M. Th., & Guschlbauer, W. (1973) *Eur. J. Biochem. 34*, 232.
Sobell, H. M., Tsai, C.-C., Gilbert, S. G., Jain, S. C., & Sakore, T. D. (1976) *Proc. Natl. Acad. Sci. U.S.A. 73*, 3068–3072.
Taylor, R., & Kennard, O. (1982) *J. Am. Chem. Soc. 104*, 3209–3212.
Teitelbaum, H., & Englander, S. W. (1975a) *J. Mol. Biol. 92*, 55–78.
Teitelbaum, H., & Englander, S. W. (1975b) *J. Mol. Biol. 92*, 79–92.
Thomas, J. C., & Schurr, J. M. (1983) *Biochemistry 22*, 6194–6198.
Thomas, T. J., & Bloomfield, V. A. (1983) *Nucleic Acids Res. 11*, 1919–1930.
Tirado, M. M., & Garcia de la Torre, J. (1980) *J. Chem. Phys. 73*, 1986–1993.
Tjerneld, F. (1982) Ph.D. Thesis, Chalmers University of Technology, Goteborg, Sweden.
Wang, A. H. J., Quigley, G. J., Kolpak, F. J., Crawford, J. L., Van Boom, J. H., Van der Marel, G., & Rich, A. (1979) *Nature (London) 282*, 680–686.
Wang, A. H. J., Quigley, G., Kolpak, F., Van der Marel, G., Van Boom, J., & Rich, A. (1981) *Science (Washington, D.C.) 211*, 171–176.
Williams, D. R. (1972) *Chem. Rev. 72*, 203–213.
Wing, R., Drew, H., Takano, T., Broka, C., Tanaka, S., Itakura, K., & Dickerson, R. E. (1980) *Nature (London) 287*, 755–758.
Wittebort, R. J., & Szabo, A. (1978) *J. Chem. Phys. 69*, 1722–1736.
Woessner, D. E. (1962) *J. Chem. Phys. 37*, 647–654.
Woessner, D. E., Snowden, B. S., & Meyer, G. H. (1969) *J. Chem. Phys. 50*, 719–721.
Wright, J. M., Feigon, J., Denny, W. A., Leupin, W., & Kearns, D. R. (1981) *J. Magn. Reson. 45*, 514–519.
Wu, H. M., Dattagupta, N., & Crothers, D. M. (1981) *Proc. Natl. Acad. Sci. U.S.A. 78*, 6808–6811.

Reactions of the Intervening Sequence of the *Tetrahymena* Ribosomal Ribonucleic Acid Precursor: pH Dependence of Cyclization and Site-Specific Hydrolysis†

Arthur J. Zaug, Jeffrey R. Kent,‡ and Thomas R. Cech*
Department of Chemistry and Biochemistry, University of Colorado, Boulder, Colorado 80309
Received April 24, 1985

ABSTRACT: During self-splicing of the *Tetrahymena* rRNA precursor, the intervening sequence (IVS) is excised as a unique linear molecule and subsequently cyclized. Cyclization involves formation of a phosphodiester bond between the 3′ end and nucleotide 16 of the linear RNA, with release of an oligonucleotide containing the first 15 nucleotides. We find that the rate of cyclization is independent of pH in the range 4.7–9.0. A minor site of cyclization at nucleotide 20 is characterized. Cyclization to this site becomes more prominent at higher pHs, although under all conditions examined it is minor compared to cyclization at nucleotide 16. The circular IVS RNAs are unstable, undergoing hydrolysis at the phosphodiester bond that was formed during cyclization. We find that the rate of site-specific hydrolysis is first order with respect to hydroxide ion concentration, with a rate constant 10^3–10^4-fold greater than that of hydrolysis of strained cyclic phosphate esters. On the basis of these results, we propose that circular IVS RNA hydrolysis involves direct attack of OH^- on the phosphate at the ligation junction, that particular phosphate being made particularly reactive by the folding of the RNA molecule. Cyclization, on the other hand, appears to occur by direct attack of the 3′-terminal hydroxyl group of the linear IVS RNA without prior deprotonation.

Splicing of the rRNA precursor of *Tetrahymena* occurs by a series of transesterification (phosphoester transfer) reactions (Cech et al., 1981; Cech, 1983). The phosphodiester bond energy is conserved in such reactions, which explains the lack of a requirement for ATP or GTP hydrolysis. Splicing is mediated by the structure of the RNA and requires no enzyme or other protein, at least in vitro (Kruger et al., 1982). It now appears that mitochondrial rRNA splicing in *Neurospora* and yeast follows the transesterification mechanism (Garriga &

† This work was supported by Grant NP-374 from the American Cancer Society. T.R.C. is the recipient of Research Career Development Award CA00700 from the National Cancer Institute, Department of Health and Human Services.
‡ Present address: Baylor College of Medicine, Houston, TX 77030.

0006-2960/85/0424-6211$01.50/0